

**DEUTSCHES ELEKTRONEN – SYNCHROTRON**

DESY 91-121

October 1991



**Production of  $D_s^+$  Mesons in B Decays  
and Determination of  $f_{D_s}$**

The ARGUS Collaboration

ISSN 0418-9833

**NOTKESTRASSE 85 · D - 2000 HAMBURG 52**

**DESY behält sich alle Rechte für den Fall der Schutzrechtserteilung und für die wirtschaftliche Verwertung der in diesem Bericht enthaltenen Informationen vor.**

**DESY reserves all rights for commercial use of information included in this report, especially in case of filing application for or grant of patents.**

**To be sure that your preprints are promptly included in the  
HIGH ENERGY PHYSICS INDEX,  
send them to the following (if possible by air mail):**

**DESY  
Bibliothek  
Notkestrasse 85  
D-2000 Hamburg 52  
Germany**

## Production of $D_s^+$ Mesons in B Decays and Determination of $f_{D_s}$

The ARGUS Collaboration

H. Albrecht, H. Ehrlichmann, T. Hamacher, A. Krüger, A. Nau, A. Nippe, M. Reidenbach,  
M. Schäfer, H. Schröder, H. D. Schulz, F. Seifow, R. Würth  
*DESY, Hamburg, Germany*

R. D. Appuhn, C. Hast, G. Herrera, H. Kolanoski, A. Lange, A. Lindner, R. Maankel, M. Schieber,  
T. Siegmund, B. Spaan, H. Thurn, D. Töpfer, A. Walther, D. Wegener  
*Institut für Physik<sup>1</sup>, Universität Dortmund, Germany*

M. G. Paulini, K. Reim, U. Volland, H. Wegener  
*Physikalisches Institut<sup>2</sup>, Universität Erlangen-Nürnberg, Germany*

R. Mündt, T. Oest, W. Schmidt-Parzefall  
*II. Institut für Experimentalphysik, Universität Hamburg, Germany*

W. Funk, J. Stiewe, S. Werner  
*Institut für Hochenergiephysik<sup>3</sup>, Universität Heidelberg, Germany*

S. Ball, J. C. Gabriel, C. Geyer, A. Hölcher, W. Hofmann, B. Holzer, S. Khan, K. T. Knöpfle,  
J. Spengler  
*Maz-Planck-Institut für Kernphysik, Heidelberg, Germany*

*Institut für Physik, Universität Karlsruhe, Germany*

D. I. Britton<sup>4</sup>, C. E. K. Charlesworth<sup>5</sup>, K. W. Edwards<sup>6</sup>, H. Kapitza<sup>6</sup>, P. Krieger<sup>6</sup>, R. Kutschke<sup>6</sup>,  
D. B. MacFarlane<sup>4</sup>, R. S. Orr<sup>4</sup>, F. M. Patel<sup>4</sup>, J. D. Prentice<sup>5</sup>, S. C. Seidel<sup>5</sup>, G. Tsipolitis<sup>4</sup>,  
K. Tsamanidaki<sup>4</sup>, R. G. Van de Water<sup>5</sup>, T.-S. Yoon<sup>5</sup>  
*Institute of Particle Physics<sup>7</sup>, Canada*

D. Reifing, S. Schael, K. R. Schubert, K. Strahl, R. Waldi, S. Weseler  
*Institut für Experimentelle Kernphysik<sup>8</sup>, Universität Karlsruhe, Germany*

B. Bošjančić, G. Kerner, P. Križan, E. Križanič, T. Podobnik, T. Živko  
*Institut J. Stefan and Oddelok za fiziko<sup>9</sup>, Univerza v Ljubljani, Ljubljana, Slovenia*

H. I. Cronström, L. Jönsson  
*Institute of Physics<sup>10</sup>, University of Lund, Sweden*

V. Balagura, M. Danilov, A. Dronskoy, B. Forninykh, A. Golutvin, I. Gorelov, F. Ratnikov,  
V. Lubimov, P. Pakhlov, A. Rostovtsev, A. Semenov, S. Semenov, V. Shevchenko<sup>11</sup>, V. Soloshenko,  
I. Tichomirov, Yu. Zaitsev  
*Institute of Theoretical and Experimental Physics, Moscow, USSR*

R. Childers, C. W. Darden  
*University of South Carolina<sup>12</sup>, Columbia, SC, USA*

<sup>1</sup> Supported by the German Bundesministerium für Forschung und Technologie, under contract number 054D051P.

<sup>2</sup> Supported by the German Bundesministerium für Forschung und Technologie, under contract number 054ER12P.

<sup>3</sup> Supported by the German Bundesministerium für Forschung und Technologie, under contract number 054HD21P.

<sup>4</sup> McGill University, Montreal, Quebec, Canada.

<sup>5</sup> University of Toronto, Toronto, Ontario, Canada.

<sup>6</sup> Carleton University, Ottawa, Ontario, Canada.

<sup>7</sup> Supported by the Natural Sciences and Engineering Research Council, Canada.

<sup>8</sup> Supported by the German Bundesministerium für Forschung und Technologie, under contract number 054KA17P.

<sup>9</sup> Supported by the Department of Science and Technology of the Republic of Slovenia and the Internationales Büro KfA.

<sup>10</sup> Supported by the Swedish Research Council.

<sup>11</sup> Deceased.

<sup>12</sup> Supported by the U.S. Department of Energy, under contract DE-AS05-80ER10690.

## Abstract

The production of  $D_s^+$  mesons in B meson decays, and in  $q\bar{q}$  continuum events, has been studied with the ARGUS detector at the  $e^+e^-$  storage ring DORIS II. In addition to the measurement of inclusive  $D_s^+$  production in  $Y(4S) \rightarrow B\bar{B}$  decays, all eight two-body decay modes  $B \rightarrow D_s^{(*)}D^{(*)}$  have been measured with branching ratios between 1% and 3%. By comparing our inclusive and exclusive results to predictions of heavy quark effective theory, a value of  $(267 \pm 28) \text{ MeV} \times [2.7\% / BR(D_s^+ \rightarrow \phi\pi^+)]^{1/2}$  is obtained for the weak decay constant  $f_{D_s^{(*)}}$ , averaged over  $D_s^+$  and  $D_s^{*+}$  mesons.

## 1 Introduction

Weak decays of B mesons are well suited to test theoretical models of heavy flavour decays and to improve our understanding of the effective quark couplings described by the unitary Cabibbo-Kobayashi-Maskawa (CKM) matrix [1]. So far less than about 12% of the exclusive hadronic decay modes of the B meson have been observed. Moreover, these measurements are mainly confined to  $B \rightarrow D^{(*)}n\pi$  and  $B \rightarrow J/\psi K^{(*)}$  transitions [2,3]. A special class of B meson decays are the exclusive double-charm channels which occur via a  $W \rightarrow c\bar{s}$  coupling in the decay chain  $b \rightarrow cW$ . Figure 1a) displays an example of such a two-body B decay produced by a spectator diagram, where the  $c\bar{s}$  quark pair hadronizes into a  $D_s^+$  or  $D_s^{*+}$  meson<sup>1</sup> and the second charm quark forms a  $D^{(*)}$  meson.

Recently, exclusive B decays to  $D_s^+$  final states have been reconstructed in three decay modes [4], while inclusive  $D_s^+$  production has already been studied in previous publications [5,6]. The measurement of exclusive B decays into  $D_s^+$  final states is also of interest since the weak decay constant of the  $D_s^+$  meson,  $f_{D_s}$ , can be derived by comparing the measured branching ratios to theoretical models describing weak decays. The decay constant is a measure of the probability that both constituent quarks of the meson annihilate to form a W boson. Thus it reflects basic dynamical properties of a bound  $q\bar{q}$  system related to its size. Knowledge of meson decay constants is essential for the extraction of fundamental CKM parameters from many weak decay processes, including  $B^0\bar{B}^0$  mixing.

In this paper an update of the ARGUS measurement [6] of inclusive  $D_s^+$  production in B decays, as well as in  $q\bar{q}$  continuum events, is reported. This analysis is presented in section 3, preceded in section 2 by a short description of the data selection. The main part of the publication is devoted to the measurement of exclusive hadronic B decays into  $D_s^+$  and D mesons, which is described in section 4. The measurement of the branching ratios of all eight decay modes  $B \rightarrow D_s^{(*)}D^{(*)}$  provides a test of the predictions of various models describing heavy meson decays. By comparing our results with two theoretical models, the weak decay

<sup>1</sup>References in this paper to a specific charged state also imply the charge conjugate state.

constant  $f_{D_s^*}$ , averaged over  $D_s^+$  and  $D_s^{*+}$ , is derived in section 5. Finally our conclusions are summarized in section 6.

## 2 Data Samples and Event Selection Procedure

The data sample used for these studies was obtained with the ARGUS detector at the  $e^+e^-$  storage ring DORIS II at centre-of-mass energies on the  $\Upsilon(4S)$  resonance and in the nearby continuum. An integrated luminosity of 246 pb $^{-1}$  was collected on the  $\Upsilon(4S)$  resonance, which corresponds to about 209 000 decays  $\Upsilon(4S) \rightarrow B\bar{B}$  assuming that the  $\Upsilon(4S)$  resonance decays only to a  $B\bar{B}$  pair. The  $q\bar{q}$  continuum sample comprises an integrated luminosity of 109 pb $^{-1}$ . The ARGUS detector, its trigger and particle identification capabilities are described in detail elsewhere [7].

Multihadron events are selected by requiring at least three tracks with either a common main vertex or a total energy deposition in the shower counters of more than 1.7 GeV. The identification of charged hadrons is based on momentum and energy loss ( $dE/dx$ ) measurements in the main drift chamber and on time-of-flight (TOF) measurement. A relative likelihood for the possible mass hypotheses  $e, \mu, \pi, K, p$  is calculated for each charged particle on the basis of this information [7]. For a given particle, all hypotheses with a likelihood ratio greater than 1% are accepted. Lepton identification combines additional information from the electromagnetic calorimeter and the muon chambers in computing the likelihood ratio.

Good particle identification and geometric acceptance are assured by requiring all particles to have a polar angle  $\theta$  with respect to the beam axis within the region  $|\cos\theta| < 0.92$ . In addition, only photons with an energy deposition in the calorimeter of at least 60 MeV are considered. All combinations of two photons with an invariant mass between 100 MeV/ $c^2$  and 170 MeV/ $c^2$  are accepted as  $\pi^0$  candidates. Energetic  $\pi^0$  mesons, whose decay photons often merge into a single cluster in the electromagnetic calorimeter, are included in the analysis by considering all shower clusters with an energy greater than 800 MeV as  $\pi^0$  candidates.  $K_S^0$  mesons are reconstructed from their  $\pi^+\pi^-$  decay forming a secondary vertex. The invariant  $\pi^+\pi^-$  mass is required to lie within  $\pm 30$  MeV/ $c^2$  of the nominal  $K_S^0$  mass [8].

## 3 Inclusive $D_s^+$ Production

The study of inclusive  $D_s^+$  production is based on the decay mode  $D_s^+ \rightarrow \phi\pi^+$ . Those  $K^+K^-$  candidates with an invariant mass within  $\pm 12$  MeV/ $c^2$  of the nominal  $\phi$  mass [8] are accepted as  $\phi$  candidates and combined with all charged pions in the event. Since the  $D_s^+$  has spin zero, the distribution of  $\cos\theta_\phi$ , the angle between the  $\phi$  direction and the  $D_s^+$  boost direction in the  $D_s^+$  rest frame, is expected to be isotropic. Random background from combinations

of soft pions with the  $\phi$  candidates peaks towards  $\cos\theta_\phi = 1$  and is suppressed by requiring  $\cos\theta_\phi < 0.8$ . Likewise, the transition of the pseudoscalar  $D_s^+$  to the vector-pseudoscalar final state  $\phi\pi^+$  results in a  $\cos^2\theta_K$  distribution, where  $\theta_K$  is the helicity angle of one kaon in the  $\phi$  rest frame with respect to the  $\pi^+$  [6]. An efficient background rejection of 50% is achieved by demanding  $|\cos\theta_K| > 0.5$ , while the signal is only reduced by 12.5%.

Shown in Figure 2 is the  $\phi\pi^+$  invariant mass distribution for  $\Upsilon(4S)$  data with the requirement that the scaled momentum  $x_p$  of the candidates be less than 0.5, where  $x_p = p_{\phi\pi}/p_{\text{max}}$  and  $p_{\text{max}} = \sqrt{E_{\text{beam}}^2 - m_\phi^2}$ . The histogram is the corresponding distribution for  $q\bar{q}$  continuum data scaled by the ratio of luminosities. A prominent peak in the  $D_s^+$  mass region can be seen. A fit using a Gaussian for the signal and a background which falls like  $1/m$  finds a  $D_s^+$  mass of  $(1967.3 \pm 1.2)$  MeV/ $c^2$  and a mass resolution  $\sigma = (10.2 \pm 1.1)$  MeV/ $c^2$ , consistent with Monte Carlo estimates. The Cabibbo-suppressed decay  $D^+ \rightarrow \phi\pi^+$ , also visible in Fig. 2, lies at a fitted mass of  $(1867.5 \pm 3.9)$  MeV/ $c^2$ , in agreement with the nominal  $D^+$  mass [9].

### 3.1 Inclusive $D_s^+$ Production in Nonresonant $q\bar{q}$ Continuum Events

The momentum distribution of  $D_s^+$  mesons is obtained by fitting the  $\phi\pi^+$  invariant mass spectrum in bins of the scaled momentum  $x_p$ . The efficiency corrected distribution for  $D_s^+$  mesons produced in nonresonant  $q\bar{q}$  continuum events is shown in Fig. 3a). The result of a fit using the Peterson fragmentation function [9]

$$f(x_p) = \frac{a}{x_p} \cdot \left( 1 - \frac{1}{x_p} - \frac{\epsilon}{1 - x_p} \right)^{-2} \quad (1)$$

with free normalization,  $a$ , and shape parameter,  $\epsilon$ , is indicated by the solid line. The statistical precision of the result is improved by using  $\Upsilon(4S)$  data for  $x_p > 0.5$  (Fig. 3b), which is beyond the kinematic limit for  $D_s^+$  production in  $B$  decays. The combined fit gives  $\epsilon = (10.8 \pm 1.5) \times 10^{-2}$ , where the normalizations of the  $\Upsilon(4S)$  and continuum data are treated as two independent free parameters. In comparison, the corresponding  $x_p$  distributions of  $D^0$  and  $D^+$  mesons are found to be softer with Peterson parameters  $\epsilon_{D^0} = (25 \pm 3) \times 10^{-2}$  and  $\epsilon_{D^+} = (19 \pm 4) \times 10^{-2}$  [10], respectively. This might be an indication that the fraction of higher excited  $D_s^+$  states, like  $D_{s^*}^{*+}$ , decaying into a  $D_s^+$  is small.

The  $D_s^+$  production cross section,  $\sigma(\epsilon^+e^- \rightarrow D_s^+X) \cdot BR(D_s^+ \rightarrow \phi\pi^+)$ , is determined from the integral of the fitted curve in Fig. 3a) to be  $(7.5 \pm 0.8 \pm 0.7)$  pb, at an averaged centre-of-mass energy of 10.5 GeV. Note, that no radiative corrections are taken into account. This result is in good agreement with our previous measurement [11]. The systematic error includes uncertainties in the luminosity calculation, the fitting procedure and the efficiency correction, respectively.

### 3.2 Inclusive $D_S^+$ Production in Decays of $B$ Mesons

The inclusive rate for  $D_S^+$  production in  $B$  meson decays is obtained by subtracting the continuum contribution from the  $\Upsilon(4S)$  data (Fig. 3b). The shape of the continuum distribution from the combined fit of the Peterson fragmentation function is used for this purpose. The resulting efficiency corrected momentum spectrum for  $D_S^+$  mesons from  $B$  decays is shown in Fig. 4. Integrating this result and dividing by the number of  $B$  mesons in the sample, the product of branching ratios,  $BR(B \rightarrow D_S^+ X) \cdot BR(D_S^+ \rightarrow \phi\pi^+)$ , is found to be  $(2.92 \pm 0.39 \pm 0.31) \times 10^{-3}$ . The uncertainties in the continuum subtraction, the efficiency correction and the number of  $B$  mesons are included in the systematic error. This determination agrees well with the CLEO results [4,5] and our previous measurement [6].

In two-body decays, such as the double-charm modes  $B \rightarrow D_S^{(*)}D^{(*)}$ , the daughter particles have a fixed momentum in the parent rest frame. Since  $B$  mesons are produced almost at rest in  $\Upsilon(4S)$  decays, the initially monochromatic momentum spectrum of the  $D_S^+$  mesons is not substantially Doppler broadened. The effects of cascade decays, where  $B \rightarrow D_S^{(*)}D^{(*)}$  and then  $D_S^{(*)} \rightarrow D_S^+\gamma$ , and detector resolution, result in only a small additional smearing of the spectrum. The observed distribution with the enhancement around  $x_p \sim 0.3$  (Fig. 4) clearly indicates the presence of such two-body decay modes. To determine the relative fraction of  $B \rightarrow D_S^{(*)}D^{(*)}$  channels, distributions are generated for the decays  $B \rightarrow D_S^+D$ ,  $B \rightarrow D_S^{*+}D$ ,  $B \rightarrow D_S^+D^*$ ,  $B \rightarrow D_S^{*+}D^*$ , with relative portions taken from the predictions of the Bauer-Stech-Wirbel (BSW) model [12]. The sum of the contribution from the four two-body decay modes is indicated in Fig. 4 by the dotted curve. The dashed line represents the sum of various three-body decay processes  $B \rightarrow D_S^{(*)}D^{(*)}\pi/\rho/\omega$ , which were generated with equal fractions of  $\pi/\rho/\omega$ . Fitting both distributions to the measured  $x_p$  spectrum yields the solid line in Fig. 4, representing a relative contribution of two-body modes,  $BR(B \rightarrow D_S^{(*)}D^{(*)})/BR(B \rightarrow D_S^+X)$ , of  $(58 \pm 7 \pm 9)\%$ . The systematic error includes variations of different compositions of the two-body and three-body spectra. This result agrees well with the value reported by CLEO [4] and our previous publication [6].

### 4 Exclusive $B$ Decays into $D_S^{(*)}D^{(*)}$

Since the inclusive  $D_S^+$  momentum spectrum implies a strong two-body component, our search for exclusive  $B$  decays is concentrated to  $B \rightarrow D_S^{(*)}D^{(*)}$  in the modes:

$$\begin{aligned} B^+ &\rightarrow D_S^+\bar{D}^0 & B^0 &\rightarrow D_S^+D^- \\ &\rightarrow D_S^{*+}\bar{D}^0 & &\rightarrow D_S^{*+}D^- \\ &\rightarrow D_S^+\bar{D}^{*0} & &\rightarrow D_S^+D^{*-} \\ &\rightarrow D_S^{*+}\bar{D}^{*0} & &\rightarrow D_S^{*+}D^{*-}. \end{aligned}$$

Small branching ratios and efficiencies require that many channels are used in reconstructing  $D$  mesons as follows:

$$\begin{aligned} D_S^{*+} &\rightarrow D_S^+\gamma & D_S^+ &\rightarrow \phi\pi^+ & D^0 &\rightarrow K^-\pi^+ & D^+ &\rightarrow K^-\pi^+\pi^+ \\ D^{*+} &\rightarrow D^0\pi^+ & &\rightarrow \phi\pi^+\pi^0 & &\rightarrow K^-\pi^+\pi^0 & &\rightarrow K^-\pi^+\pi^+\pi^0 \\ D^0 &\rightarrow D^0\pi^0 & &\rightarrow \phi\pi^+\pi^+\pi^- & &\rightarrow K^-\pi^+\pi^+\pi^- & &\rightarrow K_S^0\pi^+ \\ &\rightarrow D^0\gamma & &\rightarrow K_S^0K^+ & &\rightarrow K_S^0\pi^+\pi^- & & \\ & & &\rightarrow K_S^0K^{*+} & & & & \\ & & &\rightarrow \bar{K}^{*0}K^+ & & & & \\ & & &\rightarrow \bar{K}^{*0}K^{*+} & & & & \\ & & &\rightarrow \eta/\pi^+ & & & & \end{aligned}$$

with the subsequent decays  $\phi \rightarrow K^+K^-$ ,  $\bar{K}^{*0} \rightarrow K^-\pi^+$ ,  $K^{*+} \rightarrow K_S^0\pi^+$ ,  $\eta' \rightarrow \rho^0\gamma$ ,  $\rho^0 \rightarrow \pi^+\pi^-$ . To improve momentum resolution a mass constraint fit is applied to all intermediate states having a natural width much smaller than the detector resolution ( $K_S^0$ ,  $\pi^0$ ,  $\eta$ ,  $D_S^+$ ,  $D^0$ ,  $D^+$ ,  $D_S^{*+}$ ,  $D^{*+}$ , and  $D^{*0}$ ).

$D_S^+$ ,  $D^0$ , and  $D^+$  candidates are required to have an invariant mass within  $\pm 30$  MeV/ $c^2$ ,  $\pm 25$  MeV/ $c^2$ , and  $\pm 20$  MeV/ $c^2$  of their nominal value [8] for two-body, three-body, and four-body decays, respectively. For the decays  $D_S^+ \rightarrow \phi\pi^+\pi^0$  and  $D^0 \rightarrow K^-\pi^+\pi^0$  the corresponding mass cut was  $\pm 35$  MeV/ $c^2$ . The channels  $D_S^+ \rightarrow \phi\pi^+\pi^0$ ,  $D_S^+ \rightarrow \eta\pi^+$  and  $D^0 \rightarrow K^-\pi^+\pi^0$ , which involve neutral particles, suffer from a large combinatorial background. Therefore, they are only used for the reconstruction of the two-body modes  $B^0 \rightarrow D_S^+D^{*-}$  and  $B^+ \rightarrow D_S^+D^{*+}$ , where the  $B$  signal is particularly clean due to the excellent mass resolution for the  $D^{*+}$  signal.  $D^{*+}$  candidates are selected with an invariant mass within  $\pm 3$  MeV/ $c^2$  of the table value [8]. The reconstruction of the channel  $D_S^+ \rightarrow \eta\pi^+$  was performed using angle cuts similar to those described in detail in Ref. [13]. For the  $D_S^+$  decaying to a vector and a pseudoscalar ( $D_S^+ \rightarrow \phi\pi^+$ ,  $D_S^+ \rightarrow \bar{K}^{*0}K^+$ ,  $D_S^+ \rightarrow K^{*+}K_S^0$ ) the helicity angle distribution is also exploited as described in the inclusive study.

Selected  $D_S^{*+}$  candidates are required to have a mass difference,  $m(D_S^+\gamma) - m(D_S^+)$ , lying in the interval from 100 MeV/ $c^2$  to 180 MeV/ $c^2$ . In addition to select  $D^{*0}$  candidates within

$\pm 22$  MeV/ $c^2$  of the nominal  $D^{*0}$  mass, background from slow random neutrals is further suppressed by the requirement that the angle  $\alpha$ , defined as the  $\pi^0/\gamma$  direction with respect to the  $D^{*0}$  boost direction in the  $D^{*0}$  rest frame, satisfy  $\cos \alpha > -0.5$ . A similar restriction was applied to the  $\pi^0$  in the decay  $D^+ \rightarrow K^- \pi^+ \pi^+ \pi^0$ .

In the search for  $B$  candidates, the following additional criteria are required. The energy  $E$  of candidates for  $B \rightarrow D_s^+ D^{(*)}$  must lie within  $\pm 3\sigma_E$  of the beam energy, where  $\sigma_E$  is the experimentally-determined energy resolution. Since the combinatorial background is larger in the channels  $B \rightarrow D_s^+ D^{(*)}$  due to the soft photon in the decay  $D_s^{*+} \rightarrow D_s^+ \gamma$ , a more restrictive requirement of  $|E - E_{\text{beam}}| < 2\sigma_B$  is applied there. Mass resolution is improved for all  $B$  meson candidates through use of a kinematic fit which constrains their energy to the beam energy. For further details concerning this procedure see e.g. Ref. [2].

Background from continuum events is suppressed by using the angle  $\delta$  between the thrust axis of the  $B$  candidate and the thrust axis of all remaining particles in the event. For  $\Upsilon(4S) \rightarrow B\bar{B}$  decays this distribution should be isotropic, whereas continuum events are peaked at  $|\cos \delta| = 1$ . Events are selected with  $|\cos \delta| < 0.8$  for  $B \rightarrow D_s^+ D^{(*)}$  and  $|\cos \delta| < 0.7$  for  $D_s^+ D^{(*)}$  candidates. In addition, the momentum of the  $D$  mesons is restricted to lie below the appropriate kinematic limit for  $B$  decays, i.e.  $p_{D_s^{(*)}}$  or  $p_{D^{(*)}} < 2.0$  GeV/ $c$ , and  $p_{D_s^+}$  or  $p_{D^+} < 1.9$  GeV/ $c$  for the  $D_s^+ D^{(*)}$  modes only. Since the  $\Upsilon(4S)$  is a  $J^{PC} = 1^{--}$  state, and is produced transversely polarized, a  $\sin^2 \theta$  distribution is expected for the production angle  $\theta$  of the  $B$  mesons with respect to the beam axis. This fact is exploited to reduce random  $D_s^{(*)} D^{(*)}$  combinations by requiring  $|\cos \theta| < 0.75$ .

Finally, all  $D_s^{(*)} D^{(*)}$  combinations with a mass greater 5.15 GeV/ $c^2$  are considered as  $B$  candidates. Particularly in channels with neutral particles where a large combinatorial background can occur, events may contain more than one  $B$  candidate in a given decay mode. Multiple counting is avoided by accepting only the one  $B$  candidate per decay channel per event which has the largest total probability calculated from the sum of all  $\chi^2$  contributions from particle identification and kinematic fits. Studies show that no cross talk arises between different  $B$  decay channels, including those involving corresponding  $D_s^{*+}$  and  $D_s^+$  modes, using the described selection criteria.

#### 4.1 $B$ Meson Masses and Branching Ratios

After application of all selection criteria, the invariant mass distribution for the eight two-body decay modes  $B \rightarrow D_s^{(*)} D^{(*)}$  shown in Fig. 5 is obtained. A clear peak in the  $B$  mass region around 5.28 GeV/ $c^2$  is seen, above a low level of background. Fitting a constant to parametrize the background plus a Gaussian for the signal gives  $(25.6 \pm 5.6)$   $B$  candidates at a mass of  $(5279.5 \pm 1.1)$  MeV/ $c^2$ . The fitted mass resolution of the signal is  $\sigma_m = (4.7 \pm$

1.1) MeV/ $c^2$ , consistent with estimates from Monte Carlo studies. Applying the same analysis to our continuum data sample yields the distribution displayed as hatched histogram in Fig. 5. Scaling the continuum distribution to the  $\Upsilon(4S)$  luminosity, a background of  $(2.3 \pm 0.9)$  events is expected in the  $B$  signal region  $(5.27 \text{ GeV}/c^2 - 5.29 \text{ GeV}/c^2)$ , while the fitted constant results in  $(3.5 \pm 0.8)$  events. Thus, the background in our sample arises mainly from the  $q\bar{q}$  continuum. As a further check that our  $B$  candidates originate from  $\Upsilon(4S) \rightarrow B\bar{B}$  decays, the polar angle distribution for those candidates with a mass greater than 5.27 GeV/ $c^2$  is found to be consistent with the expected  $\sin^2 \theta$  behaviour. In addition, the angle between the thrust axes of the  $B$  candidate and the remainder of the event is compatible with an isotropic distribution, as expected for  $\Upsilon(4S) \rightarrow B\bar{B}$  decays.

Dividing our  $B$  candidates sample into neutral and charged  $B$  mesons (Fig. 6) allows a determination of their separate masses:

$$m_{B^0} = (5278.1 \pm 1.7 \pm 2.0) \text{ MeV}/c^2$$

$$m_{B^+} = (5280.8 \pm 1.4 \pm 2.0) \text{ MeV}/c^2.$$

The systematic error includes the uncertainties on the mass of the  $\Upsilon(4S)$  resonance, the determination of the beam energy, and the background parametrization. These values correspond to a mass difference between the neutral and charged  $B$  meson of

$$m_{B^0} - m_{B^+} = (-2.7 \pm 2.2 \pm 1.2) \text{ MeV}/c^2,$$

which is in good agreement with our previous result [2]. Note, within the given statistics the method to choose only one  $B$  candidate per decay channel per event has no influence on the  $B^0/B^+$  masses, but may not be negligible with better statistics.

In Fig. 7 the mass distributions for our candidates are shown separately for the eight two-body decay modes

$$\begin{aligned} \text{a) } & B^+ \rightarrow D_s^+ \bar{D}^0, \text{ b) } B^+ \rightarrow D_s^+ \bar{D}^0, \text{ c) } B^+ \rightarrow D_s^+ \bar{D}^{*0}, \text{ d) } B^+ \rightarrow D_s^+ \bar{D}^{*0}, \\ \text{e) } & B^0 \rightarrow D_s^+ D^-, \text{ f) } B^0 \rightarrow D_s^+ D^-, \text{ g) } B^0 \rightarrow D_s^+ D^{*-}, \text{ h) } B^0 \rightarrow D_s^+ D^{*-}. \end{aligned}$$

Each mode has entries in the  $B$  mass region as well as some background events. To determine the number of signal events for a particular channel a fit is performed with a constant to account for the background plus a Gaussian for the signal. The mass of the latter is fixed to the mean of the measured  $B$  mass and the width is set to the value estimated from Monte Carlo studies. By this procedure the number of events in the  $B$  signal region as well as the background expectation is obtained for each decay mode and listed in Table 1.

Reconstruction efficiencies are determined using simulated  $\Upsilon(4S) \rightarrow B\bar{B}$  decays with one  $B$  meson decaying to a  $D_s^{(*)} D^{(*)}$  channel. The events are passed through a detailed detector simulation and the ARGUS reconstruction program. The branching ratios of the

charmed mesons are taken from [8], where the  $BR(D^0 \rightarrow K^- \pi^+)$ ,  $BR(D^+ \rightarrow K^- \pi^+ \pi^+)$ , and  $BR(D^{*+} \rightarrow D^0 \pi^+)$  are stated to be  $(3.71 \pm 0.25)\%$ ,  $(7.7 \pm 1.0)\%$ , and  $(55 \pm 4)\%$ , respectively. Since  $D_S^+$  branching ratios are only reliably known relative to  $BR(D_S^+ \rightarrow \phi \pi^+)$ , large errors on the absolute scale result from the uncertainty in the latter. For this study, a fixed value of 2.7% was assumed for  $BR(D_S^+ \rightarrow \phi \pi^+)$  as taken from [8]. The values obtained for the  $B$  decay branching ratios are listed in Table 1. The quoted systematic errors include uncertainties in the number of  $B$  mesons produced, the  $D$  and  $D^*$  branching ratios, the fitting procedure used to derive the number of signal events, and the efficiency determination. However, no contribution is included from the overall scale error on  $BR(D_S^+ \rightarrow \phi \pi^+)$ . Furthermore, it is assumed that charged and neutral  $B$  mesons are equally produced in  $\Upsilon(4S)$  decays, since the mass difference is found to be zero within the experimental uncertainty, and that decays of the  $\Upsilon(4S)$  to non- $B\bar{B}$  states are negligible.

Our measured branching ratios for the decays  $B^+ \rightarrow D_S^+ \bar{D}^0$ ,  $B^0 \rightarrow D_S^+ D^-$ , and  $B^0 \rightarrow D_S^+ D^{*-}$  are in good agreement with the CLEO results [4], if they are scaled to  $BR(D_S^+ \rightarrow \phi \pi^+) = 2.7\%$  (see Tab. 1). For all other decay modes we found evidence for the first time. The sum of the measured  $B \rightarrow D_S^{(*)} D^{(*)}$  branching ratios almost doubles the fraction of known hadronic  $B^0$  and  $B^+$  branching ratios.

#### 4.2 Discussion of Results and Comparison with Theoretical Predictions

As a check, the measured branching ratios for the decays  $B \rightarrow D_S^{(*)} D^{(*)}$  can be compared to the results of our inclusive study. The sum of all four exclusive decay modes yields a two-body branching ratio of  $(8.4 \pm 2.6)\%$  for  $B^+ \rightarrow D_S^{*+} \bar{D}^{*0}$  and  $(8.4 \pm 3.0)\%$  for  $B^0 \rightarrow D_S^{*+} D^{*-}$ . From the inclusive measurement of the product of branching ratios, the total  $B$  rate into  $D_S^+$  mesons is  $BR(B \rightarrow D_S^+ X) = (10.8 \pm 1.8)\%$ , using the same value of 2.7% for the  $BR(D_S^+ \rightarrow \phi \pi^+)$ . Taking the value of  $(58 \pm 11)\%$  from the fit to the momentum distribution in the inclusive study gives a  $BR(B \rightarrow D_S^{(*)} D^{(*)})$  of  $(6.3 \pm 1.6)\%$ . This is somewhat smaller, but still consistent within errors with the sum of the exclusive two-body decay modes.

The measured branching ratios can be used to estimate the lifetime ratio  $\tau(B^+)/\tau(B^0)$  of charged and neutral  $B$  mesons. With  $\tau(B^+)/\tau(B^0) \approx BR(B^+ \rightarrow D_S^{*+} \bar{D}^{*0})/BR(B^0 \rightarrow D_S^{*+} D^{*-})$  we obtain  $\tau(B^+)/\tau(B^0) = 1.0 \pm 0.4$ , in good agreement with previous measurements [14,15].

Our results can be compared with predictions from several existing theoretical models describing weak hadronic decays of heavy flavour mesons. This is most easily done by considering ratios of branching ratios, where there is a cancellation of assumptions concerning  $D_S^+$  and  $D$  branching ratios on the experimental side, and  $V_{cb}$ ,  $\tau_B$ , and in particular  $f_{D_S}$

used in various theoretical predictions. The ratios  $BR(B^+ \rightarrow D_S^{*+} \bar{D}^0)/BR(B^+ \rightarrow D_S^+ \bar{D}^0)$ ,  $BR(B^+ \rightarrow D_S^{*+} \bar{D}^0)/BR(B^+ \rightarrow D^0 \pi^+)$ ,  $BR(B^0 \rightarrow D_S^{*+} D^-)/BR(B^0 \rightarrow D_S^+ D^-)$ , and  $BR(B^0 \rightarrow D_S^{*+} D^-)/BR(B^0 \rightarrow D_S^+ D^{*-})$  are shown in Figure 8, along with the corresponding predictions from the models of Bauer-Stech-Wirbel [12] (triangles  $\Delta$ ), Körner [16] (circles  $\circ$ ), Hussain-Scadron [17] (squares  $\square$ ), and Mannel-Roberts-Ryzak [18] (diamonds  $\diamond$ ), the latter representing calculations from heavy quark effective theory. Although the errors on the measured ratios of branching ratios are large, there is still some discrimination possible between the different models. Thus, the predictions from heavy quark effective theory and the BSW model fit well to our data, while the approaches of Körner and Hussain-Scadron represent a less adequate description.

### 5 Determination of the Weak Decay Constant $f_{D_S^{(*)}}$

Theoretical models describing weak decays of heavy flavour mesons usually assume a factorization approach, which works well for semileptonic decays. Here, the leptonic current and hadronic currents decouple so that a semileptonic decay is described by a simple product of the two. It remains to be demonstrated whether the same assumption holds for hadronic two-body decays, where the leptonic current is replaced by a second hadronic term. In our case, the decay amplitude of a transition such as  $B^0 \rightarrow D_S^+ D^-$  is given by the product

$$(D^- | j_\mu | B^0) |_{q^2=m_{D_S^+}^2} \times q^\mu f_{D_S} \quad (2)$$

(see Fig. 1a), where  $f_{D_S}$  is the weak decay constant and  $q^\mu$  the four-momentum of the  $D_S^+$ . For the corresponding decay to a vector meson,  $B^0 \rightarrow D_S^+ D^-$ , eq. (2) becomes

$$(D^- | j_\mu | B^0) |_{q^2=m_{D_S^+}^2} \times \epsilon^{\mu\nu} m_{D_S^+} f_{D_S}, \quad (3)$$

where  $\epsilon^{\mu\nu}$  is the polarization vector.

The studied decays  $B \rightarrow D_S^{(*)} D^{(*)}$  are well suited to determine the decay constant of the  $D_S^+$  meson, since this transition can only occur via a  $c\bar{s}$  quark pair coupling to a  $W$  boson emitted externally in the  $b \rightarrow cW$  transition (Fig. 1a). In terms of the BSW model [12] the decay  $B \rightarrow D_S^{(*)} D^{(*)}$  is a pure  $a_1$  transition. It is not possible to produce  $D_S^+$  mesons by a so called colour-suppressed internal  $W$  emission ( $a_2$  type) (see Fig. 1b). In order to obtain an estimate of the theoretical uncertainty, two approaches, heavy quark effective theory and the BSW model, are used to determine  $f_{D_S^{(*)}}$ . Both describe our data well, and produce comparable results.

## 5.1 Determination of $f_{D_s^{(*)}}$ using Heavy Quark Effective Theory

Recently, an exciting new theoretical approach, referred to as Heavy Quark Effective Theory (HQET), has been developed to describe weak decays [19]. In the limit that the mass of the heavy quark can be considered infinitely large, the recoil of the light quark does not change the velocity of the heavy quark, causing the latter to behave as a static colour source. In this picture, the QCD interactions of the light quark are unperturbed by the transition of one heavy quark into another. An important feature of this theory is the hypothesis that all heavy meson decays are governed by one single form factor, known as the Isgur-Wise function.

Heavy quark effective theory can be combined with the factorization assumption to allow precise predictions in non-leptonic decays. Bortolotto and Stone [20] tested factorization at the 25% level by comparing the reactions  $B^0 \rightarrow \pi^+ D^{*-}$  and  $B^0 \rightarrow D^{*-} \ell^+ \nu_\ell$ . If the meson produced from the virtual  $W$  is heavy, colour transparency arguments [21] do not hold, and experimental verification of factorization in the case of the decays  $B \rightarrow D_s^{(*)} D^{(*)}$  should be obtained. Mannel, Roberts and Ryzak [22] have suggested that the ratio of widths  $\Gamma(B \rightarrow D_s^+ D^-) / \Gamma(B \rightarrow D_s^+ D^*)$  should be unity, if factorization is valid. This can be checked with our measurement. Averaging  $BR(B^+ \rightarrow D_s^+ \bar{D}^0)$  with  $BR(B^0 \rightarrow D_s^+ D^-)$ , and  $BR(B^+ \rightarrow D_s^+ \bar{D}^0)$  with  $BR(B^0 \rightarrow D_s^+ D^*)$ , the experimental value for  $\Gamma(B \rightarrow D_s^+ D^-) / \Gamma(B \rightarrow D_s^+ D^*)$  is  $1.5 \pm 1.0$ . This is compatible with unity, but is not a particularly strong test.

Heavy quark effective theory predicts equal decay rates for  $B^0 \rightarrow \pi^+ D^-$  and  $B^0 \rightarrow \pi^+ D^{*-}$ . Combining CLEO data from Ref. [3] and recent ARGUS results [2], the weighted mean values for  $BR(B^0 \rightarrow \pi^+ D^-)$  and  $BR(B^0 \rightarrow \pi^+ D^{*-})$  are in good agreement with this HQET prediction (Tab. 2). Therefore we are allowed to average the two mean values to  $BR(B^0 \rightarrow \pi^+ D^{(*)-}) = (0.37 \pm 0.05 \pm 0.08)\%$ , which is used for normalization purposes below.

In order to calculate the predictions of heavy quark effective theory for  $\Gamma(B \rightarrow D_s^{(*)} D^{(*)})$ , the following expression by Rosner [23], predicting the rate of a  $B$  decaying to a pseudoscalar  $P$  and a  $D$ , is useful:

$$\Gamma(B^0 \rightarrow PD^-) = \frac{G_F^2 f_P^2 |V_{cb}|^2 |V_{cs}|^2 m_B^3 \Lambda^3 |\xi(w_P^2)|^2 \cdot (1 - \sqrt{\zeta}) \cdot \lambda^{1/2}(1, \zeta, y_P)}{32\pi \cdot 4\sqrt{\zeta}}, \quad (4)$$

where  $\Lambda$  are QCD corrections, and  $m_B = 5.28 \text{ GeV}/c^2$ ,  $m_D = m_{D^*} = 1.97 \text{ GeV}/c^2$  (spin weighted average),  $m_P$  is the mass of the pseudoscalar,  $\zeta = (m_D/m_B)^2$ ,  $\lambda(a, b, c) = a^2 + b^2 + c^2 - 2ab - 2ac - 2bc$ ,  $y_P = (m_P/m_B)^2$  and  $\xi(w_P^2)$  is the Isgur-Wise function with  $w_P^2 = (v \cdot v')^2 = [m_P^2 - (m_B - m_P)^2] / m_B m_D$ . Using the universality of the form factor, similar expressions can be derived for the  $B$  decays to pseudoscalar-vector ( $D_s^+ D$ ,  $D_s^+ D^*$ ) and vector-vector ( $D_s^+ D^*$ ) final states. For example, neglecting  $m_{D^*} - m_D$  and using the prediction that in the heavy quark limit the spin symmetry gives  $f_{D_s} = f_{D_s^*}$ , the ratio  $\Gamma(B^0 \rightarrow D_s^+ D^-) / \Gamma(B^0 \rightarrow \pi^+ D^-)$

can be expressed with equation (4) as:

$$\frac{\Gamma(B^0 \rightarrow D_s^+ D^-)}{\Gamma(B^0 \rightarrow \pi^+ D^-)} = \frac{f_{D_s}^2}{f_\pi^2} \cdot \frac{|V_{cs}|^2}{|V_{ud}|^2} \cdot \frac{\lambda^{1/2}(1, \zeta, y_{D_s^+})}{\lambda^{1/2}(1, \zeta, y_{\pi^+})} \cdot \frac{[(1 + \sqrt{\zeta})^2 - y_{D_s^+}]^2}{[(1 + \sqrt{\zeta})^2 - y_{\pi^+}]^2}, \quad (5)$$

where we set  $V_{cs} = V_{ud}$  and take  $f_\pi = 132 \text{ MeV}$  from [8].

There are several proposals for an analytical form for the Isgur-Wise function in recent literature. Three different expressions are used for comparison and as an indication of the systematic uncertainty introduced by choosing a specific form. Rosner has suggested [23] a simple pole hypothesis:

$$\xi(w^2) = \frac{1}{1 - \frac{w^2}{w_0^2}}, \quad (6)$$

while Mannel, Roberts and Ryzak [18] give the parametrization

$$\xi(w^2) = \exp\{\kappa \cdot w^2\}. \quad (7)$$

A new method for calculating the Isgur-Wise function from hadronic form factors at maximum recoil has been proposed by Neubert and Rieckert [24]. In their treatment, which can be generalized to incorporate the leading mass corrections in the heavy quark limit,  $\xi(w^2)$  is:

$$\xi(w^2) = \frac{1}{1 - w^2/4} \cdot \exp\left\{\beta \cdot \frac{w^2}{4 - w^2}\right\}. \quad (8)$$

Common to all three expressions is a free parameter ( $w_0, \kappa$  or  $\beta$ ) which must be fixed by reference to data. This is achieved using measurements of semileptonic  $B$  decays, such as the average semileptonic branching fractions  $BR(B \rightarrow D\ell\nu)$  and  $BR(B \rightarrow D^*\ell\nu)$ , which have been rescaled in Table 3 to reflect a consistent set of charm branching ratios from [8], used within this paper. The values for  $w_0, \kappa$  or  $\beta$  listed in Table 4 are obtained by simultaneously fitting the ratios  $BR(B \rightarrow D\ell\nu) / BR(B^0 \rightarrow \pi^+ D^{(*)-})$ ,  $BR(B \rightarrow D^*\ell\nu) / BR(B^0 \rightarrow \pi^+ D^{(*)-})$ , and the polarization variable  $\alpha = 2\Gamma_L / \Gamma_T - 1$  taken from Ref. [25,26].

Using the values for the free parameters so obtained, the weak decay constants  $f_{D_s}$  and  $f_{D_s^*}$  are extracted by comparing the theoretical predictions of  $BR(B \rightarrow D_s^+ D^{(*)-}) / BR(B^0 \rightarrow \pi^+ D^{(*)-})$  and  $BR(B \rightarrow D_s^+ D^{(*)}) / BR(B^0 \rightarrow \pi^+ D^{(*)-})$  with our measurements of the corresponding branching ratios  $B \rightarrow D_s^{(*)} D^{(*)}$  and the averaged value for  $BR(B^0 \rightarrow \pi^+ D^{(*)-})$ . The resulting decay constants  $f_{D_s}$  and  $f_{D_s^*}$ , obtained by this procedure, are listed in Table 4. The systematic errors reflect the uncertainties in the fitted parameters  $w_0, \kappa$  or  $\beta$ . As expected in the heavy quark limit [18] both decay constants are equal on the 20% level within errors. Averaging over the  $D_s^+$  and  $D_s^{*+}$  mesons the values for  $f_{D_s^{(*)}}$ , also listed in Table 4, are obtained. Since the variation of the result with different forms of the Isgur-Wise function is small, a mean value of  $f_{D_s^{(*)}} = (273 \pm 32 \pm 14) \text{ MeV} \times [2.7\% / BR(D_s^+ \rightarrow \phi\pi^+)]^{1/2}$  is quoted from our exclusive measurement.



Our inclusive measurement  $BR(B \rightarrow D_s^+ X) \cdot BR(D_s^+ \rightarrow \phi\pi^+) = (2.92 \pm 0.50) \times 10^{-3}$  can also be used to obtain a value for  $f_{D_s^{(*)}}$ . Using the result from the fit to the momentum spectrum that  $(58 \pm 11)\%$  of inclusive  $D_s^+$  mesons are produced in two-body decays, and assuming that  $BR(D_s^+ \rightarrow \phi\pi^+) = 2.7\%$ , a value of  $(6.3 \pm 1.6)\%$  is obtained for  $BR(B \rightarrow D_s^{(*)} D^{(*)})$ . Thus, the ratio  $BR(B \rightarrow D_s^{(*)} D^{(*)})/BR(B^0 \rightarrow \pi^+ D^{(*)-})$  implies a value of  $f_{D_s^{(*)}} = (255 \pm 45 \pm 13) \text{ MeV} \times [2.7\%/BR(D_s^+ \rightarrow \phi\pi^+)]^{1/2}$ , in good agreement with the result extracted from the exclusive measurement. Since the inclusive and exclusive results are almost independent, a final weighted average of

$$f_{D_s^{(*)}} = (267 \pm 28) \text{ MeV} \times [2.7\%/BR(D_s^+ \rightarrow \phi\pi^+)]^{1/2},$$

is obtained, where the statistical and systematic errors are added in quadrature.

## 5.2 Determination of $f_{D_s^{(*)}}$ using the BSW Model

The second method is to extract  $f_{D_s^{(*)}}$  from a comparison between our measured branching ratios for  $B \rightarrow D_s^{(*)} D^{(*)}$  and the predictions of the BSW model which successfully describes other exclusive hadronic  $B$  meson decays [2]. It is again advantageous to consider the ratios of widths  $\Gamma(B \rightarrow D_s^+ D^{(*)})/\Gamma(B^0 \rightarrow \pi^+ D^{(*)-})$  and  $\Gamma(B \rightarrow D_s^+ D^{(*)})/\Gamma(B^0 \rightarrow \pi^+ D^{(*)-})$ , respectively. The BSW predictions have been rescaled in terms of  $f_{D_s}$  and  $f_{D_s^*}$  according to the values used in Ref. [12], while other quantities, such as  $a_1$ ,  $V_{cb}$  and  $\tau_B$ , cancel in the ratio.

The measured ratios  $\Gamma(B \rightarrow D_s^{(*)} D^{(*)})/\Gamma(B^0 \rightarrow \pi^+ D^{(*)-})$  are taken from the averaged branching ratios  $BR(B^0 \rightarrow \pi^+ D^-) = (0.37 \pm 0.06 \pm 0.08)\%$  and  $BR(B^0 \rightarrow \pi^+ D^{*-}) = (0.36 \pm 0.07 \pm 0.08)\%$  from Table 2. From a fit of the four measurements,  $\Gamma(B^+ \rightarrow D_s^+ \bar{D}^0)/\Gamma(B^0 \rightarrow \pi^+ D^-)$ ,  $\Gamma(B^0 \rightarrow D_s^+ D^-)/\Gamma(B^0 \rightarrow \pi^+ D^-)$ ,  $\Gamma(B^+ \rightarrow D_s^+ \bar{D}^{*0})/\Gamma(B^0 \rightarrow \pi^+ D^{*-})$ , and  $\Gamma(B^0 \rightarrow D_s^+ D^{*-})/\Gamma(B^0 \rightarrow \pi^+ D^{*-})$  to the corresponding theoretical predictions of the BSW model,  $f_{D_s}$  is determined to be  $(331 \pm 55) \text{ MeV} \times [2.7\%/BR(D_s^+ \rightarrow \phi\pi^+)]^{1/2}$ . Substituting a  $D_s^{*+}$  for the  $D_s^+$  in these decay processes, the corresponding four ratios imply  $f_{D_s^*} = (280 \pm 46) \text{ MeV} \times [2.7\%/BR(D_s^+ \rightarrow \phi\pi^+)]^{1/2}$ . Thus, the results derived by using the BSW model are in agreement with these from heavy quark effective theory.

This agreement might be expected in the light of a recent paper by Neubert et al. [27], who relate and compare the hadronic form factor approach of the BSW model [12] to the predictions of heavy quark effective theory, and find that both give similar results. This shows that from the perspective of HQET the parametrization of the form factors in the original BSW ansatz was chosen in a very intuitive and successful way.

## 6 Conclusion

In summary, the production of  $D_s^+$  mesons in decays of  $B$  mesons, and in  $q\bar{q}$  continuum events, has been studied. From the measurement of the  $D_s^+$  momentum distribution in nonresonant  $q\bar{q}$  continuum events, the production cross-section is calculated to be  $\sigma(e^+e^- \rightarrow D_s^+ X) \times BR(D_s^+ \rightarrow \phi\pi^+) = (7.5 \pm 0.8 \pm 0.7) \text{ pb}$  with a Peterson fragmentation parameter  $\epsilon = (10.8 \pm 1.5) \times 10^{-2}$ . The measured momentum distribution of  $D_s^+$  mesons from  $B$  decays implies  $BR(B \rightarrow D_s^+ X) \times BR(D_s^+ \rightarrow \phi\pi^+) = (2.92 \pm 0.39 \pm 0.31) \times 10^{-3}$ , while a fit using the BSW model yields a relative contribution of  $(58 \pm 7 \pm 9)\%$  from two-body decay channels. A search for exclusively reconstructed hadronic two-body decays finds first evidence for all eight decay modes  $B \rightarrow D_s^{(*)} D^{(*)}$ , with branching ratios between about 1% and 3%. From our inclusive and exclusive studies, the weak decay constant  $f_{D_s^{(*)}}$ , averaged over  $D_s^+$  and  $D_s^{*+}$  mesons, is determined to be  $(267 \pm 28) \text{ MeV} \times [2.7\%/BR(D_s^+ \rightarrow \phi\pi^+)]^{1/2}$  using the predictions of heavy quark effective theory. A similar result is obtained exploiting the BSW model.

In Table 5 we compare our measurement of  $f_{D_s^{(*)}}$  to theoretical predictions from potential models, bag models, QCD sum rules and lattice calculations. Their estimates range in general between 200 – 300 MeV. The values closer to 300 MeV are in agreement with our result.

Finally, we can use our determination of  $f_{D_s^{(*)}} = (267 \pm 28) \text{ MeV} \times [2.7\%/BR(D_s^+ \rightarrow \phi\pi^+)]^{1/2}$  to obtain a prediction for the leptonic decays  $D_s^+ \rightarrow l^+ \nu_l$ , where  $l^+$  stands for  $\mu^+$  or  $\tau^+$ . With the observed  $D_s^+$  lifetime [8] and the expression [23]

$$\Gamma(D_s^+ \rightarrow l^+ \nu_l) = \frac{G_F^2 f_{D_s^+}^2 |V_{cs}|^2 m_l^2 m_{D_s^+}}{8\pi} \left[ 1 - \frac{m_l^2}{m_{D_s^+}^2} \right]^2, \quad (9)$$

we estimate  $BR(D_s^+ \rightarrow \tau^+ \nu_\tau) = (4.9 \pm 0.5)\% \times [2.7\%/BR(D_s^+ \rightarrow \phi\pi^+)]$ , and  $BR(D_s^+ \rightarrow \mu^+ \nu_\mu) = (0.5 \pm 0.06)\% \times [2.7\%/BR(D_s^+ \rightarrow \phi\pi^+)]$ . Both branching ratios contribute a remarkable fraction to the total  $D_s^+$  decay width.

## Acknowledgements

It is a pleasure to thank U. Djuanda, E. Konrad, E. Michel, and W. Reinsch for their competent technical help in running the experiment and processing the data. We thank Dr. H. Neseemann, B. Sarau, and the DORIS group for the excellent operation of the storage ring. The visiting groups wish to thank the DESY directorate for the support and kind hospitality extended to them. In addition, we gratefully acknowledge fruitful discussions with Dr. T. Mannel and Dr. M. Neubert.

## References

- [1] N. Cabibbo, *Phys.Rev.Lett.* **10** (1963) 531;  
M. Kobayashi, T. Maskawa, *Prog.Theor.Phys.* **49** (1973) 652.
- [2] H. Albrecht et al. (ARGUS), *Z.Phys.* **C48** (1990) 543.
- [3] D. Cassel (CLEO), in *Proceedings of Physics in Collision 10*, Duke University, Durham, edited by A. Goshaw, L. Montanet, World Scientific, Singapore, 1990.
- [4] D. Bortoletto et al. (CLEO), *Phys.Rev.Lett.* **64** (1990) 2117.
- [5] P. Haas et al. (CLEO), *Phys.Rev.Lett.* **56** (1986) 2781.
- [6] H. Albrecht et al. (ARGUS), *Phys.Lett.* **B187** (1987) 425.
- [7] H. Albrecht et al. (ARGUS), *Nucl.Instr.Methods* **A275** (1989) 1.
- [8] Particle Data Group, *Phys.Lett.* **B239** (1990) 1.
- [9] C. Peterson et al., *Phys.Rev.* **D27** (1983) 105.
- [10] H. Albrecht et al. (ARGUS), DESY 91-023 (1991), submitted to *Z.Phys.* **C**;  
G. Harder, Ph.D. Thesis, Univ. Hamburg, DESY F15-89/01 (1989).
- [11] H. Albrecht et al. (ARGUS), *Phys.Lett.* **B207** (1988) 349.
- [12] M. Bauer, B. Stech, M. Wirbel, *Z.Phys.* **C34** (1987) 103.
- [13] H. Albrecht et al. (ARGUS), *Phys.Lett.* **B245** (1990) 315.
- [14] H. Albrecht et al. (ARGUS), *Phys.Lett.* **B232** (1989) 554;  
H. Albrecht et al. (ARGUS), DESY 91-056 (1991).
- [15] R. Fulton et al. (CLEO), *Phys.Rev.* **D43** (1991) 651.
- [16] J. G. Körner, in *Proceedings of the International Symposium on Production and Decay of Heavy Hadrons*, Heidelberg, Germany, edited by K. R. Schubert and R. Waldi, 1986.
- [17] F. Hussain, M. D. Scadron, *Phys.Rev.* **D30** (1984) 1492.
- [18] T. Mannel, W. Roberts, Z. Ryzak, *Phys.Lett.* **B259** (1991) 485.
- [19] M. Voloshin, M. Shifman, *Sov.J.Nucl.Phys.* **45** (1987) 292 and  
*Sov.J.Nucl.Phys.* **47** (1988) 511;  
E. Eichten, B. Hill, *Phys.Lett.* **B234** (1990) 511;  
H. Politzer, M. Wise, *Phys.Lett.* **B206** (1988) 681 and *Phys.Lett.* **B208** (1988) 504;  
N. Isgur, M. Wise, *Phys.Lett.* **B232** (1989) 113 and *Phys.Lett.* **B237** (1990) 527;  
B. Grinstein, *Nucl.Phys.* **B339** (1990) 253;  
H. Georgi, *Phys.Lett.* **B240** (1990) 447;  
J. D. Bjorken, SLAC preprint, SLAC-PUP-5278 (1990);  
A. Falk, H. Georgi, B. Grinstein, M. Wise, *Nucl.Phys.* **B343** (1990) 1;  
A. Falk, B. Grinstein, *Phys.Lett.* **B247** (1990) 406.
- [20] S. Stone, D. Bortoletto, *Phys.Rev.Lett.* **65** (1990) 2951.
- [21] S. J. Brodsky, in *Proceedings of Third Lake Louise Winter Institute on QCD: Theory and Experiment*, Lake Louise, Canada, edited by B. A. Campbell et al., World Scientific, New Jersey, 1988;  
M. J. Dugan, B. Grinstein, *Phys.Lett.* **B255** (1991) 583.
- [22] T. Mannel, W. Roberts, Z. Ryzak, *Phys.Rev.* **D44** (1991) 18.
- [23] J. L. Rosner, *Phys.Rev.* **D42** (1990) 3732.
- [24] M. Neubert, V. Rieckert, Heidelberg preprint, HD-THEP-91-6 (1991),  
submitted to *Nucl.Phys.* **B**.
- [25] H. Albrecht et al. (ARGUS), *Phys.Lett.* **B219** (1989) 121.
- [26] D. Bortoletto et al. (CLEO), *Phys.Rev.Lett.* **63** (1989) 1667.
- [27] M. Neubert et al., Heidelberg preprint, HD-THEP-91-28 (1991),  
to be published in *Heavy Flavours*, ed. A. J. Buras and M. Lindner,  
*Adv. Ser. on Dir. in High Energy Physics*, World Scient. Publ. Comp.
- [28] H. Albrecht et al. (ARGUS), *Phys.Lett.* **B229** (1989) 175.
- [29] H. Albrecht et al. (ARGUS), *Phys.Lett.* **B197** (1987) 452.
- [30] D. Antreasyan et al. (Crystal Ball), *Z.Phys.* **C48** (1990) 553.
- [31] H. Krasemann, *Phys.Lett.* **B96** (1980) 397.
- [32] S. Godfrey, N. Isgur, *Phys.Rev.* **D32** (1985) 189.
- [33] M. Suzuki, *Phys.Lett.* **B162** (1985) 392.

## Figure Captions

- Figure 1** Spectator diagram for a double-charm  $B$  meson decay (a) and for internal  $W$  emission (b).
- Figure 2** The  $\phi\pi^+$  invariant mass distribution for  $\Upsilon(4S)$  data (crosses) and  $q\bar{q}$  continuum events (histogram) with  $x_p < 0.5$ . The continuum distribution is scaled to reflect the luminosity ratio of the two samples. The solid curve is the result of a fit using a background falling like  $1/m$  plus two Gaussians for the  $D_S^+$  signal and the decay  $D^+ \rightarrow \phi\pi^+$ .
- Figure 3** The efficiency corrected momentum distribution for  $D_S^+$  mesons from (a) non-resonant  $q\bar{q}$  continuum events and from (b)  $\Upsilon(4S)$  data. The solid curve is the result from a combined fit of the Peterson fragmentation function to all continuum data and the  $\Upsilon(4S)$  spectrum with  $x_p > 0.5$ .
- Figure 4** The momentum spectrum of  $D_S^+$  mesons from  $B$  decays. The curves are the result of a fit of expected spectra for two-body decays  $B \rightarrow D_S^{(*)}D^{(*)}$  and three-body processes as described in the text.
- Figure 5** The invariant mass distribution for all eight decay modes  $B \rightarrow D_S^{(*)}D^{(*)}$ . The solid line is the result of a fit using a Gaussian for the signal plus a constant to parametrize the background. The corresponding distribution for the continuum data is shown as the hatched histogram (unscaled).
- Figure 6** Mass distributions of  
a) neutral  $B$  decays  $B^0 \rightarrow D_S^{(*)+}D^{(*)-}$  and  
b) charged  $B$  decays  $B^+ \rightarrow D_S^{(*)+}\bar{D}^{(*)0}$ .
- Figure 7** Separate invariant mass distributions for the decay channels  
a)  $B^+ \rightarrow D_S^+\bar{D}^0$ , b)  $B^+ \rightarrow D_S^+\bar{D}^0$ , c)  $B^+ \rightarrow D_S^+\bar{D}^{*0}$ , d)  $B^+ \rightarrow D_S^+\bar{D}^{*0}$ ,  
e)  $B^0 \rightarrow D_S^+D^-$ , f)  $B^0 \rightarrow D_S^+D^-$ , g)  $B^0 \rightarrow D_S^+D^{*-}$ , h)  $B^0 \rightarrow D_S^+D^{*-}$ .
- Figure 8** Comparison of the ratios of branching ratios  
 $BR(B^+ \rightarrow D_S^+\bar{D}^0)/BR(B^+ \rightarrow D_S^+\bar{D}^0)$ ,  
 $BR(B^+ \rightarrow D_S^+\bar{D}^{*0})/BR(B^+ \rightarrow D_S^+\bar{D}^{*0})$ ,  
 $BR(B^0 \rightarrow D_S^+D^-)/BR(B^0 \rightarrow D_S^+D^-)$  and  
 $BR(B^0 \rightarrow D_S^+D^{*-})/BR(B^0 \rightarrow D_S^+D^{*-})$  with the corresponding theoretical predictions of different models.

- [34] S. N. Sinha, Phys.Lett. **B178** (1986) 110.
- [35] P. Cea et al., Phys.Lett. **B206** (1988) 691.
- [36] D. Silverman, H. Yao, Phys.Rev. **D38** (1988) 214.
- [37] S. Capstick, S. Godfrey, Phys.Rev. **D41** (1990) 2856.
- [38] E. Golowich, Phys.Lett. **B91** (1980) 271.
- [39] V.S. Mathur, M.T. Yamawaki, Phys.Lett. **B107** (1981) 127; Phys.Rev. **D29** (1984) 2057.
- [40] C.A. Dominguez, N. Paver, Phys.Lett. **B197** (1987) 423; Phys.Lett. **B199** (1987) 596(E).
- [41] S. Narison, Phys.Lett. **B198** (1987) 104.
- [42] M.A. Shifman, Usp.Fiz.Nauk **151** (1987) 193; [Sov.Phys.Ups. **30** (1987) 91].
- [43] M.B. Gavela et al., Phys.Lett. **B206** (1988) 113.
- [44] T.A. DeGrand, R.D. Loft, Phys.Rev. **D38** (1988) 954.
- [45] C. Bernard et al., Phys.Rev. **D38** (1988) 3540.
- [46] R.M. Woloshyn et al., Phys.Rev. **D39** (1989) 978.
- [47] C. Alexandrou et al., Phys.Lett. **B256** (1991) 60.

Table 1: The branching ratios of decay modes  $B \rightarrow D_S^{(*)} D^{(*)}$ , assuming a fixed value of 2.7% for  $BR(D_S^+ \rightarrow \phi \pi^+)$ . The measurements from the CLEO collaboration [4] are scaled to the same  $D_S^+$  normalization.

$B$ decay mode	Events in $B$ mass region	Background expectation	Branching ratio	$BR$ from [4]
$B^+ \rightarrow D_S^+ \bar{D}^0$	5	$0.6 \pm 0.3$	$(2.4 \pm 1.2 \pm 0.4)\%$	$(2.4 \pm 1.1)\%$
$B^+ \rightarrow D_S^+ \bar{D}^0$	3	$0.7 \pm 0.3$	$(1.6 \pm 1.2 \pm 0.3)\%$	
$B^+ \rightarrow D_S^+ \bar{D}^{*0}$	2	—	$(1.3 \pm 0.9 \pm 0.2)\%$	
$B^+ \rightarrow D_S^+ \bar{D}^{*0}$	5	$0.2 \pm 0.1$	$(3.1 \pm 1.6 \pm 0.5)\%$	
$B^0 \rightarrow D_S^+ D^-$	3	$0.6 \pm 0.4$	$(1.7 \pm 1.3 \pm 0.6)\%$	$(1.1 \pm 0.6)\%$
$B^0 \rightarrow D_S^+ D^-$	4	$0.8 \pm 0.4$	$(2.7 \pm 1.7 \pm 0.9)\%$	
$B^0 \rightarrow D_S^+ D^{*-}$	3	$0.4 \pm 0.3$	$(1.4 \pm 1.0 \pm 0.3)\%$	$(2.0 \pm 1.2)\%$
$B^0 \rightarrow D_S^+ D^{*-}$	4	$0.1 \pm 0.1$	$(2.6 \pm 1.4 \pm 0.6)\%$	

Table 2: Exclusive two-body  $B^0$  branching ratios [%].

Mode	ARGUS	CLEO II	CLEO I	Average
$\pi^+ D^-$	$0.57 \pm 0.13 \pm 0.13$	$0.30 \pm 0.07 \pm 0.05$	$0.60 \pm 0.32 \pm 0.17$	$0.37 \pm 0.06 \pm 0.08$
$\pi^+ D^{*-}$	$0.33 \pm 0.11 \pm 0.07$	$0.42 \pm 0.11 \pm 0.08$	$0.32 \pm 0.15 \pm 0.09$	$0.36 \pm 0.07 \pm 0.08$

Table 3: Compilation of semileptonic  $B$  decay rates [%]. The values are scaled from the references given in brackets to the  $D$  branching ratios [8] used in this publication.

$BR(\bar{B}^0 \rightarrow D^+ \ell \nu)$	$1.9 \pm 0.6 \pm 0.5$ [28]	$2.1 \pm 0.7 \pm 0.4$ [15]	
$BR(B^+ \rightarrow D^0 \ell \nu)$	$1.8 \pm 0.7 \pm 0.3$ [15]		
Average			$1.9 \pm 0.4 \pm 0.4$
$BR(\bar{B}^0 \rightarrow D^{*+} \ell \nu)$	$6.4 \pm 1.1 \pm 1.7$ [29]	$5.4 \pm 0.6 \pm 0.8$ [26]	
$BR(\bar{B}^0 \rightarrow D^{*0} \ell \nu)$	$4.6 \pm 0.9^{+0.9}_{-1.0}$ [15]		
$BR(B \rightarrow D^* \ell \nu)$	$7.0 \pm 1.8 \pm 1.4$ [30]		
Average			$5.5 \pm 0.4 \pm 1.1$

Table 4: Results for the weak decay constants  $f_{D_S}$  and  $f_{D_S^*}$  using different parametrizations of the Isgur-Wise function (eqs. (6), (7), (8)). The values for  $f_{D_S^{(*)}}$  are obtained by averaging the results for  $D_S^+$  and  $D_S^{*+}$  mesons. The fitted free parameters of the Isgur-Wise functions are also listed.

	eq. (6), Ref. [23]	eq. (7), Ref. [18]	eq. (8), Ref. [24]
Free parameter	$w_0 = 1.17 \pm 0.20$	$\kappa = 0.49 \pm 0.12$	$\beta = 1.53 \pm 0.63$
Weak decay constant	in $\text{MeV} \times [2.7\% / BR(D_S^+ \rightarrow \phi \pi^+)]^{1/2}$		
$f_{D_S}$	$320 \pm 53 \pm 11$	$314 \pm 52 \pm 14$	$318 \pm 52 \pm 12$
$f_{D_S^*}$	$255 \pm 42 \pm 11$	$251 \pm 41 \pm 13$	$254 \pm 41 \pm 11$
$f_{D_S^{(*)}}$	$275 \pm 33 \pm 11$	$271 \pm 32 \pm 13$	$274 \pm 32 \pm 12$

Table 5: Compilation of some theoretical estimates for the weak decay constant  $f_{D_S}$  from potential models, bag models, sum rules and lattice calculations. The values given are in MeV.

	potential model	bag model	sum rules	lattice
210	[31]	166 [38]	$\sim 232$ [39]	$215 \pm 17$ [43]
335	[32]		$276 \pm 13$ [40]	$157 \pm 11$ [44]
91	[33]		$218 \pm 20$ [41]	$234 \pm 72$ [45]
356	[34]		$200 \pm 15$ [42]	$\sim 280$ [46]
199	[35]			$209 \pm 18$ [47]
380-590	[36]			
$290 \pm 20$	[37]			

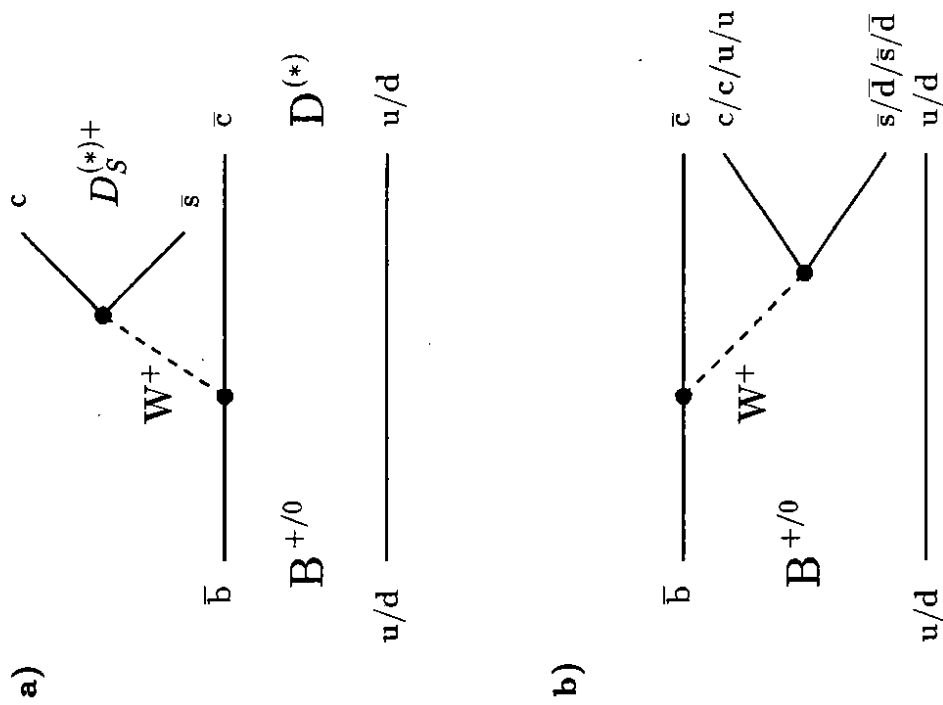


Figure 1

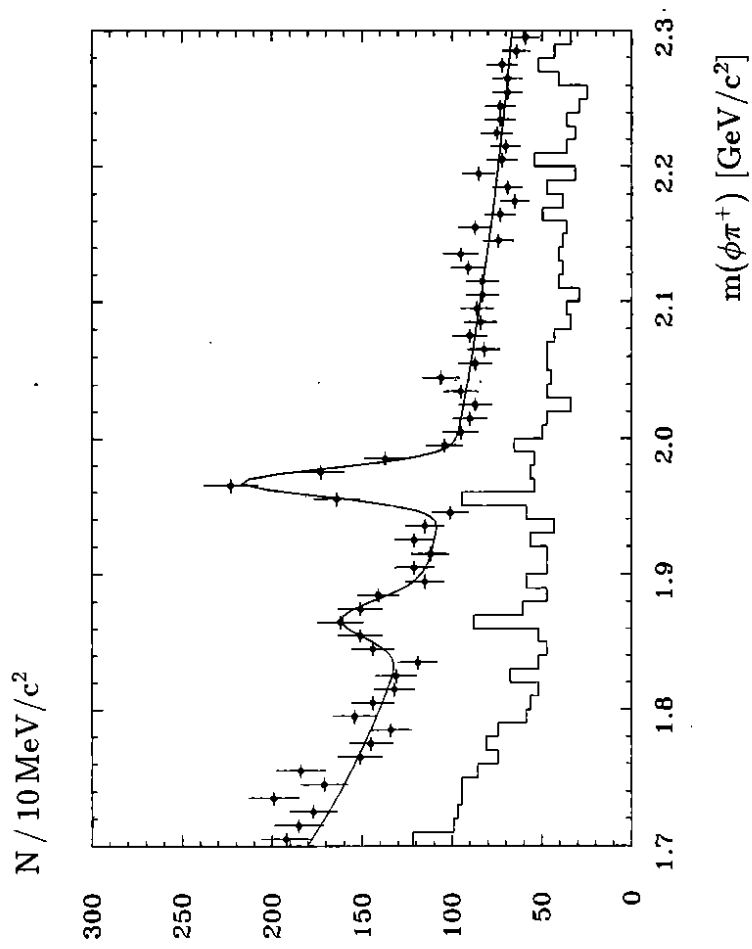


Figure 2

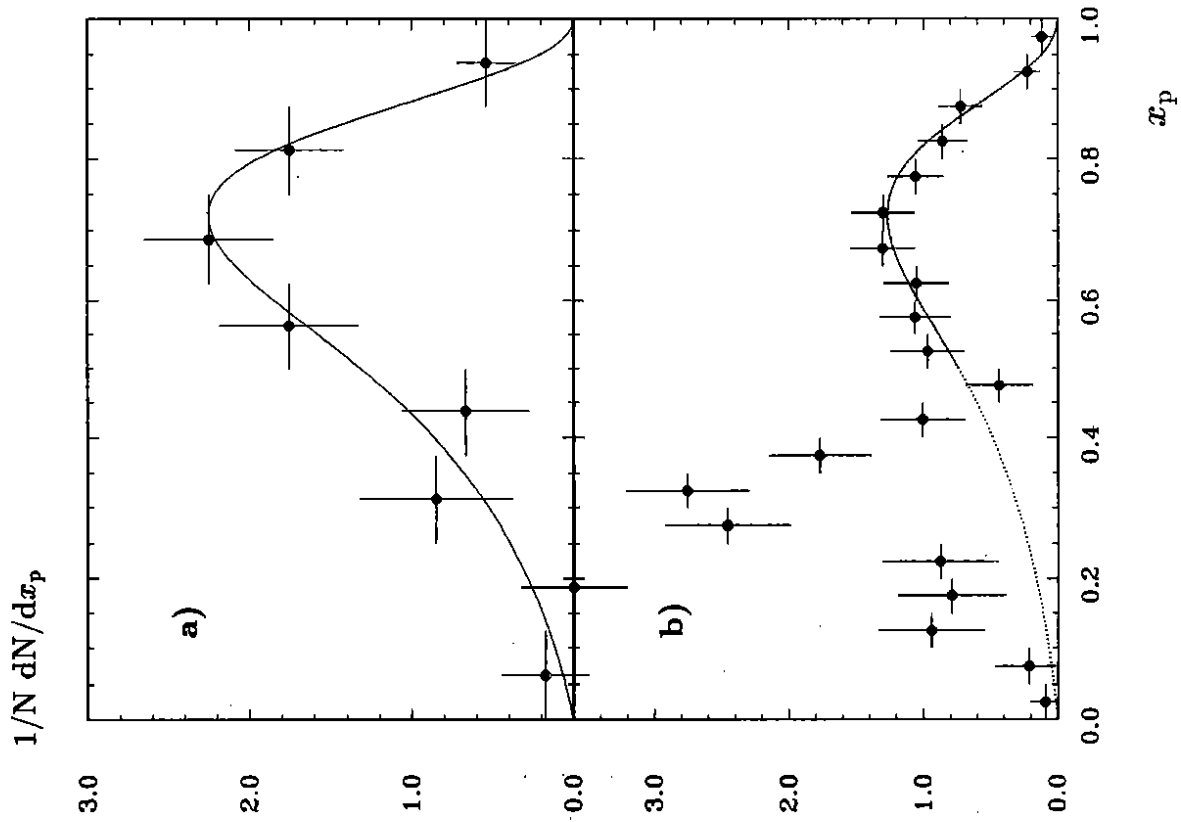


Figure 3

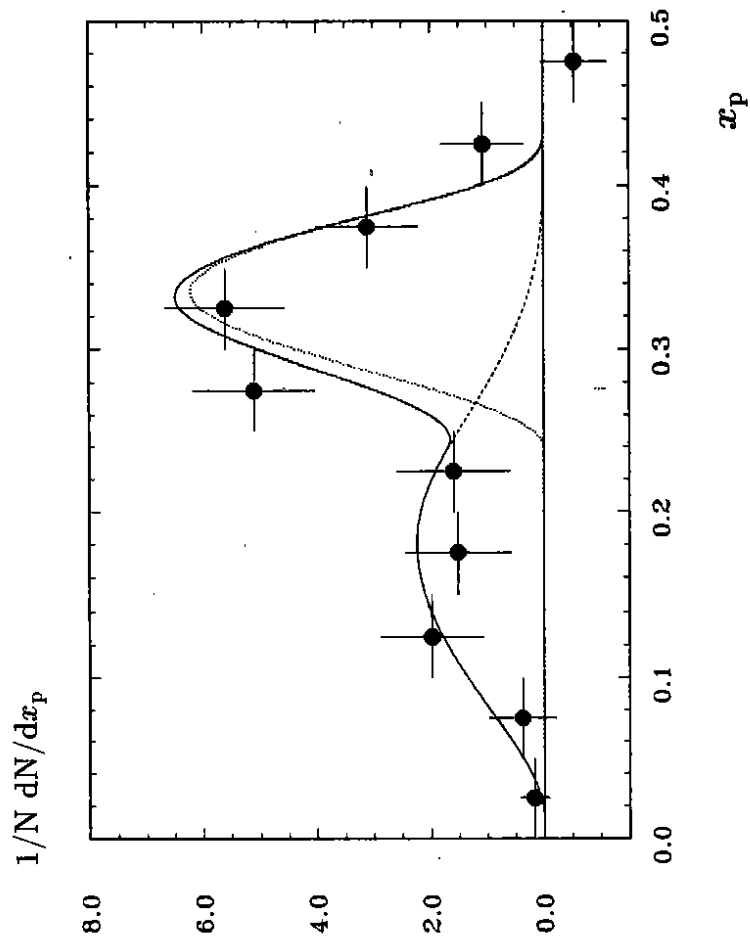


Figure 4

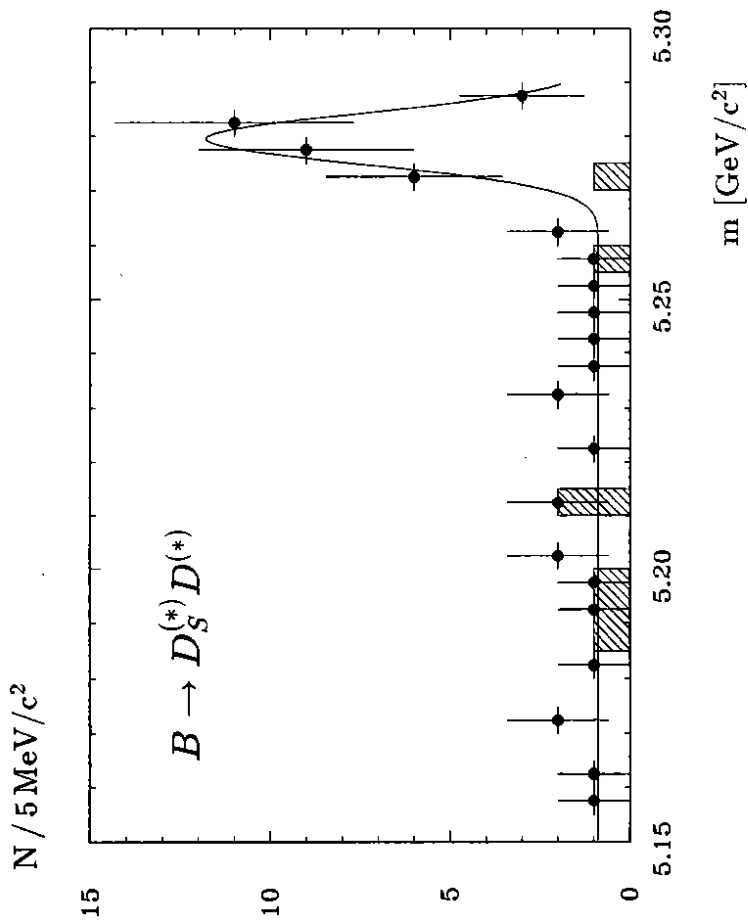


Figure 5

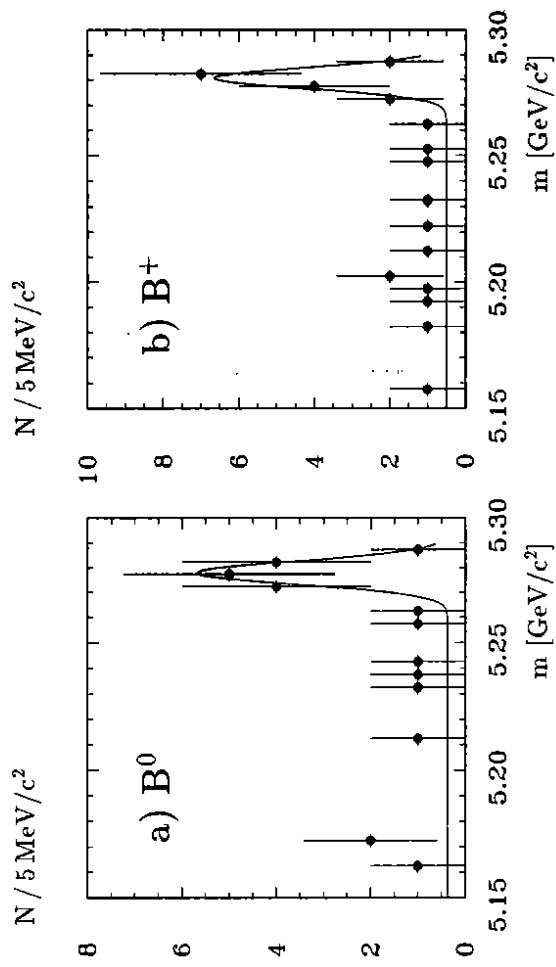


Figure 6

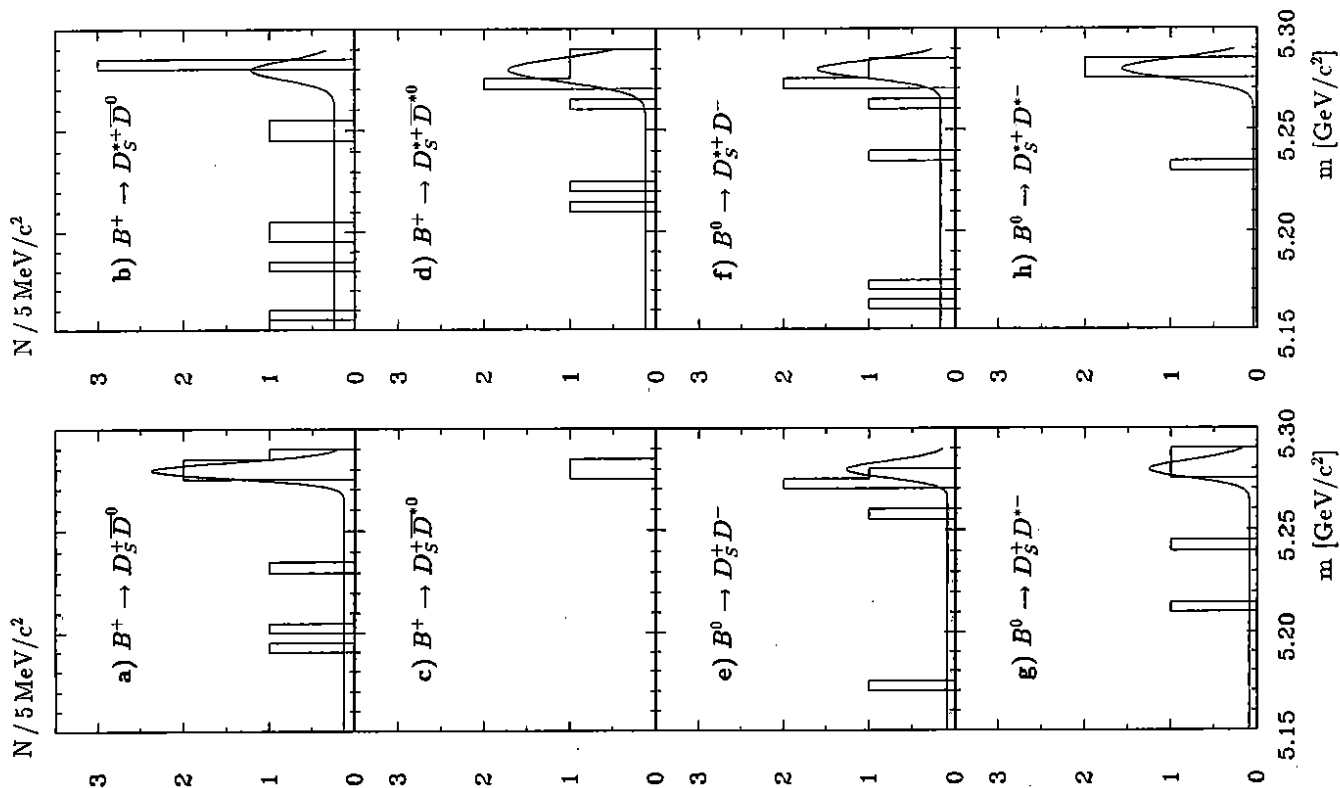


Figure 7

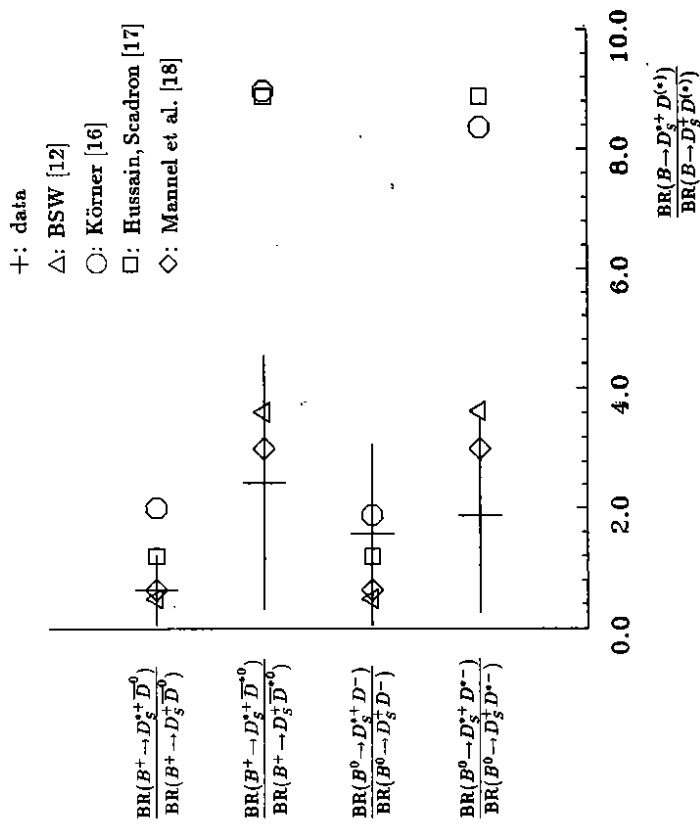


Figure 8